



A possible nonpolar solvation mechanism at an intermediate time scale: the solvent-cage expansion

S.L. Chang, Ten-Ming Wu*

Institute of Physics, National Chiao-Tung University, HsinChu, Taiwan 300, ROC

Received 6 April 2000

Abstract

Through studying the so-called ‘epsilon’ nonpolar solvation model, we propose that the expansion of the solvent cage, which is composed of the solvents at the vicinity of the first maximum of the solute-solvent radial distribution function, might be a possible solvation mechanism at a time scale between inertial motions and structural relaxation. The expansion is triggered by the strong repulsion between the solute and its neighboring solvents, originally inside the cage. This intermediate mechanism is found to be the cause for the bump following the ultrafast decay in the solvation time correlation functions of the ‘epsilon’ model at low densities. © 2000 Elsevier Science B.V. All rights reserved.

1. Introduction

Solvation dynamics plays an important role in many chemical reactions in solutions, and is generally divided into two classes: polar when the solvent molecule reorientation is predominant and nonpolar when the solvent molecule center-of-mass motion dominates. Because of the small reorganization energy, the existing experimental studies for the dynamics of nonpolar solvation [1–3] are not so many as those for polar solvation. In a recent experimental study on nonpolar solvation dynamics in terms of three-pulse photon echo [3], the results revealed three distinct solvent dynamical time scales: An ultrafast component within 100 fs and a slow component in 2–3 ps, and an intermediate component roughly at 600 fs. Similar as the cases in polar solvation [4], the

origins of the ultrafast and the slow components are, respectively, attributed to inertial motions and structural relaxation. However, the origin of the intermediate component is still unknown; a mechanistic interpretation is thus requested.

Theoretically, solvation dynamics is analyzed by studying the normalized solvation time correlation function $C(t)$, which is defined [5] as

$$C(t) = \frac{\langle \delta \Delta E(0) \delta \Delta E(t) \rangle}{\langle (\delta \Delta E)^2 \rangle}, \quad (1)$$

where ΔE is the differential solute-solvent interaction energy, caused by some external perturbation on the solute, and $\delta \Delta E = \Delta E - \langle \Delta E \rangle$ is the corresponding fluctuation. The brackets refer to an equilibrated ensemble average. In the so-called ‘epsilon’ nonpolar solvation model [6,7], in which each particle with a mass m is assumed to have two electronic states, and one particle, referred as the solute, is

* Corresponding author. Fax: (886)-03-5720728; e-mail: tmw@cc.nctu.edu.tw

excited, the ground state solute-solvent interaction is described by a Lennard–Jones (LJ) potential,

$$\phi(r) = 4\epsilon \left\{ \left(\frac{\sigma}{r} \right)^{12} - \left(\frac{\sigma}{r} \right)^6 \right\}, \quad (2)$$

and the excited state solute-solvent interaction is by another LJ potential, which has the same diameter σ , but a deeper well depth ϵ_1 . Thus, $\lambda \equiv (\epsilon_1 - \epsilon)/\epsilon$ serves as the only parameter of the model, and

$$\Delta E = \lambda \sum_{i=1}^N \phi(r_{0i}), \quad (3)$$

where r_{0i} is the distance between the solute and the i -th solvent particle. However, $C(t)$ of the ‘epsilon’ model is independent of λ . Proved by many authors [6,8], $C(t)$ of this model at low-density solvents shows a small bump arising right after the rapid decay of the ultrafast component; however, as the solvent density increases the bump gradually disappears. Calculating through molecular dynamics (MD) simulations, which will be discussed later, we present in Fig. 1 the $C(t)$ functions of this model for solvents at three different thermodynamic states. The main subject in this Letter is to study the origin to cause the bump, with the motivation that to understand the origin might give some insights about the mechanisms for the intermediate component of non-polar solvation dynamics.

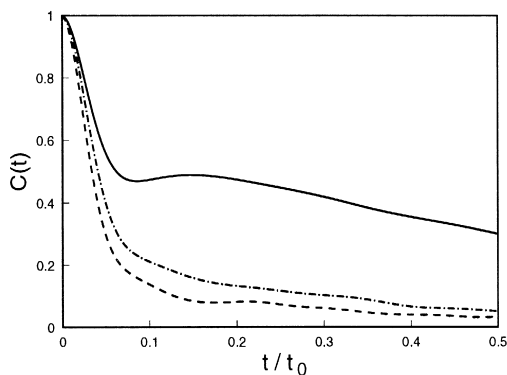


Fig. 1. The normalized solvation time correlation functions of the ‘epsilon’ solvation model at three thermodynamic states: $\rho^* = 0.5$ and $T^* = 1.41$ (solid line), $\rho^* = 0.85$ and $T^* = 1.41$ (dashed line), and $\rho^* = 0.85$ and $T^* = 1.0$ (dot-dashed line), where $\rho^* \equiv \rho\sigma^3$ and $T^* \equiv k_B T/\epsilon$ are the reduced density and temperature of the simple LJ fluid, respectively. $t_0 = (m\sigma^2/\epsilon)^{1/2}$

In methodology, we will analyze solvation dynamics described by the ‘epsilon’ model in terms of two different methods: The mean-relative-displacement (MRD) [9] and the instantaneous-normal-mode (INM) [10,11] analyses. In the former method, we focus on the relative motions of the solute-solvent pairs with their initial separations of the order of σ . The MRD analysis provides information about the effects of the solvent cage, which is referred as the solvents near the first maximum of the solute-solvent radial distribution function, on solvation dynamics. The results of this analysis indicate that the expansion of the solvent cage [12], before relaxed through diffusion processes, might be a mechanistic origin for the bump mentioned above. The solvent-cage expansion is triggered by the impulses from those solvent particles, which were originally inside the cage, but are strongly repelled out by the solute in the inertial-motion time scale. Thus, the time scale of the solvent-cage expansion is intermediate between those of inertial motion and structural relaxation. In the INM analysis, we calculate the INM solvation spectra due to the attractive and repulsive parts of the differential solute-solvent interaction. The results of the INM analysis support the possibility of the solvent-cage expansion.

2. Mean-relative-displacement analysis

In general, $C(t)$ depends on the relative motions of the solute-solvent pairs [6], rather than the single-particle motions. To describe the relative motions of atomic pairs in fluids, we have recently developed a quantity, called the mean relative displacement [9], denoted as $U(\mathbf{r}, t)$, which is defined as the ensemble average of the relative displacements at time t of the atomic pairs, given that their initial separation vectors were \mathbf{r} . $U(\mathbf{r}, t)$ actually describes the displacement from \mathbf{r} of the average center of the time-dependent conditional probability $G_2(\mathbf{r}, \mathbf{r}'; t)$ [13] for finding those initially specified atomic pairs with separation vectors to be \mathbf{r}' at time t . In a uniform simple liquid, $U(\mathbf{r}, t)$ has only the component parallel to \mathbf{r} , denoted as $U^{\parallel}(\mathbf{r}, t)$, which depends only on $r \equiv |\mathbf{r}|$. A detail of the MRD analysis on the relative motions of atomic pairs in a low-density simple LJ

fluid is given in Ref. [9], in which the radial spreading of the $G_2(\mathbf{r}, \mathbf{r}'; t)$ distribution was also examined. The results indicate that up to the time scale of the bump in the $C(t)$ function shown in Fig. 1, the relative motions of atomic pairs are resolvable through the MRD analysis, and several conclusions were given. Within the inertial-motion time scale, those particles having separations from a central particle about r_m , the distance corresponding to the first maximum of the radial distribution function, tend to retain their separations with respect to the central one, since the mean forces on them are almost zero. However, those nearest neighbors of the central particle are repelled out of r_m in the inertial-motion time scale due to the strong repulsive forces from the central particle.

In this section, in terms of the MRD analysis, we study the ‘epsilon’ solvation model in a limiting case, in which the parameter λ is taken to be infinitesimally small, since $C(t)$ of the ‘epsilon’ model is independent of λ . The limiting case of the ‘epsilon’ model is virtually a simple LJ fluid, which is an easier system to do MD simulations. The details of our simulations are given in Ref. [9]. We have performed the MD simulations for the simple LJ system at three thermodynamic conditions, and calculated their $C(t)$ functions, which are presented in Fig. 1.

The MRD results for those three LJ fluids are shown in Fig. 2 by plotting $d(r, t) = r + U^{\parallel}(r, t)$, the averaged separation at time t between two atoms, as functions of t for several different values of r . In Fig. 2, we have changed the reference frame for describing the relative motions of atomic pairs from the frame fixed in the laboratory to the one moving with an atom, which is taken to be the solute. The meaning of the reference-frame change is that by taking the solute as the origin we examine how its neighbors move relative to it. Shown in Fig. 2, the chosen initial neighbors of the solute are from the nearest to the solute to those with separations larger than r_m . For all of the three states, those solvent particles with initial separations near r_m are more stable relative to the solute, due to the almost-vanished mean forces on them, and form a metastable cage around the solute. This metastable cage serves a boundary to divide the solvents into two parts: inside and outside. The relative motions to the solute for

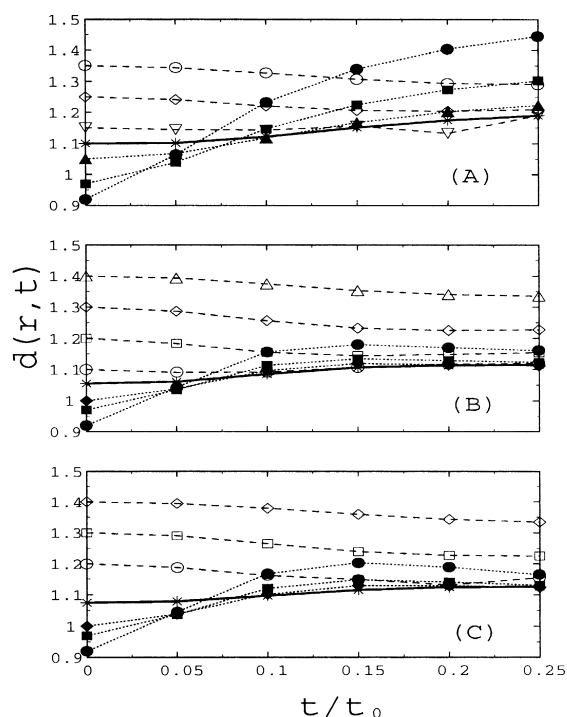


Fig. 2. The averaged separations $d(r, t)$ between two atoms in a fluid as functions of t for three thermodynamic states of the LJ fluid: $\rho^* = 0.5$ and $T^* = 1.41$ (A), $\rho^* = 0.85$ and $T^* = 1.41$ (B), and $\rho^* = 0.85$ and $T^* = 1.0$ (C). In each plot, the symbols are the MD simulation results, and connected with the bold solid line, the dotted lines and the dashed lines for r , the initial separations of the two atoms, equal to, smaller than and larger than the distance of the first maximum of the radial distribution function, respectively.

the solvents in the two parts behave quite differently. Due to the shielding of the cage, the short-time motions of the solvents initially outside the cage are not much influenced by the solute. On the contrary, those solvent particles initially inside the cage feel strong repulsive forces from the solute and are repelled out of the cage in a very short time scale. After carefully checking on Figs. 1 and 2, we found several interesting observations, which are given in the following:

(A) For particles originally inside the cage (with $r < r_m$), the closer a particle to the solute is, the earlier the particle is scattered out of the cage.

(B) For all of the three states, only after those particles originally inside the cage pass through r_m ,

those particles initially near r_m tend to move outwardly. However, the average outward movements are significant in the low-density fluid, but small in the two high-density fluids.

(C) For the fluid ($\rho^* = 0.5$), whose $C(t)$ function has a bump, the time scale for those particles originally inside the cage passing through r_m is roughly of the order of the time ($\approx 0.086t_0$) for $C(t)$ decaying to a minimum before the bump shows up.

The first observation is easily understood from the fact that as two neighboring particles get closer the repulsive force between them is stronger. A reasonable interpretation for the second observation is that the outward movements of those particles initially near r_m are due to the impulses from the passing through of those solvent particles originally in the innermost part of the cage. Thus, before the time scale of structural relaxation, this average outward movement can be recognized as an expansion of the solvent cage. The rigidity of the cage, which depends on solvent density, certainly influences its expansion. The cage is expected to expand easily in a low-density solvent, but hard, or even prohibited, in a high-density one. This expectation agrees with our second observation.

In the third observation, we connect the MRD analysis with the $C(t)$ function for the solvent at $\rho^* = 0.5$. Before passing through r_m , the particles originally inside the cage have similar behaviors relative to the solute for the three solvents shown in Fig. 2. However, after passing through r_m , in the low-density solvent, these particles keep on moving outwardly in general, with their average movements having no returns up to the time scale of the bump, but, in the two high-density solvents, these particles seem to be trapped in the solvent-cage region. Therefore, a possible explanation for the arising of the bump is the expansion of the cage before the particles composed of the cage diffuse away so that the metastable cage is relaxed. This explanation also gives a reason why no bump is seen in the $C(t)$ function of a high-density fluid. Due to the rigidity of the fluid structure, the cage in a high-density fluid is prohibited to expand significantly to produce a bump in the $C(t)$ function before the relaxation of the cage. In the next section, we will justify our explanation on the arising of the bump through the INM analysis.

3. Instantaneous-normal-mode analysis

The details of the INM analysis on short-time dynamics of solvation have been given in some articles [14–16]. Here, we only give a summary. In the linearized INM theory of solvation, Stratt and Cho [14] have shown that the normalized solvation time correlation function can be written as

$$C(t) = 1 - \frac{k_B T}{\langle (\delta \Delta E)^2 \rangle} \int d\omega \rho_{\text{solv}}(\omega) \frac{(1 - \cos \omega t)}{\omega^2}, \quad (4)$$

where the solvation spectrum $\rho_{\text{solv}}(\omega)$ is given by the weighted INM density of states (DOS)

$$\rho_{\text{solv}}(\omega) = \left\langle \sum_{\alpha=1}^{3N} \left(\frac{\partial \Delta E}{\partial q_\alpha} \right)^2 \delta(\omega - \omega_\alpha) \right\rangle, \quad (5)$$

with $\partial \Delta E / \partial q_\alpha$ to be the linear coupling coefficient as ΔE modulated by the INM coordinate q_α with frequency ω_α in a configuration. Up to t^2 , the short-time expansion of $C(t)$ is given as

$$C(t) = 1 - \frac{1}{2} \omega_{\text{solv}}^2 t^2 + \dots, \quad (6)$$

where the square of the solvation frequency ω_{solv} is

$$\omega_{\text{solv}}^2 = \frac{k_B T}{\langle (\delta \Delta E)^2 \rangle} \int \rho_{\text{solv}}(\omega) d\omega. \quad (7)$$

The solvation spectrum is a crucial quantity in the linearized INM solvation theory. With the same solvation model we study here, Stratt and coworkers [16] have shown that the major contribution (more than 80%) to the solvation spectrum comes from the nearest solvent particle of the solute. With this result, they suggested that the solute-solvent binary modes, the instantaneous vibrational motions between the mutual-nearest solute-solvent pairs [17], be responsible for the high-frequency solvation spectrum, and dominates the short-time dynamics of solvation. While it is a good idea to simplify the complicated many-particle solvation dynamics to the binary modes, the relative motions of the mutual-nearest solute-solvent pairs do not fully account for the whole solvation spectrum, especially the low-frequency part, which means that a few more solvent

particles should be included to give a more accurate description on short-time dynamics of solvation.

In the ‘epsilon’ model, the differential solute-solvent interaction, which is a LJ potential, is repulsive and attractive for the solvent particles inside and outside the solvent cage, respectively, in case that we ignore the small difference between r_m and the minimum of the LJ potential, caused by the added linear term in potential in our MD simulations [9]. In order to examine the contribution of the solvent particles inside or outside the cage to the solvation spectrum, we divide the LJ potential at $2^{1/6}\sigma$ so that the differential solute-solvent interaction is separated into the repulsive and attractive parts. With this separation, the solvation energy ΔE is a sum of two contributions, ΔE_{in} and ΔE_{out} , which are due to the repulsive and attractive parts of the differential solute-solvent interaction, respectively. Correspondingly, $C(t)$ is a sum of four components.

$$C(t) = C_{\text{in-in}}(t) + C_{\text{out-out}}(t) + C_{\text{in-out}}(t) + C_{\text{out-in}}(t), \quad (8)$$

$$C_{\mu\nu}(t) = \frac{\langle \delta \Delta E_{\mu}(t) \delta \Delta E_{\nu}(0) \rangle}{\langle (\delta \Delta E)^2 \rangle}, \quad (9)$$

where the indices μ and ν can be either ‘in’ or ‘out’, and $\delta \Delta E_{\mu} = \Delta E_{\mu} - \langle \Delta E_{\mu} \rangle$. $C_{\text{in-in}}(t)$ and $C_{\text{out-out}}(t)$ are, respectively, the responses at time t from the solvent particles inside and outside the division at $2^{1/6}\sigma$. $C_{\text{in-out}}(t)$ and $C_{\text{out-in}}(t)$, which are equal due to time reversal, are the cross-term correlation functions for solvent particles inside the division and those particles outside. In the linearized INM solvation theory, the unnormalized $C_{\mu\nu}(t)$ function can be approximated with a formula similar as Eq. (5), except for changing the leading constant to be $\langle \delta \Delta E_{\mu}(0) \delta \Delta E_{\nu}(0) \rangle / \langle (\delta \Delta E)^2 \rangle$, and replacing the solvation spectrum with the following one

$$\rho_{\text{solv}}^{\mu\nu}(\omega) = \left\langle \sum_{\alpha=1}^{3N} \frac{\partial \Delta E_{\mu}}{\partial q_{\alpha}} \frac{\partial \Delta E_{\nu}}{\partial q_{\alpha}} \delta(\omega - \omega_{\alpha}) \right\rangle. \quad (10)$$

The physical meaning of $\rho_{\text{solv}}^{\mu\nu}(\omega)$ is straightforward. $\rho_{\text{solv}}^{\text{in-in}}(\omega)$ and $\rho_{\text{solv}}^{\text{out-out}}(\omega)$ are, respectively, the solvation spectra arising solely from the solvent parti-

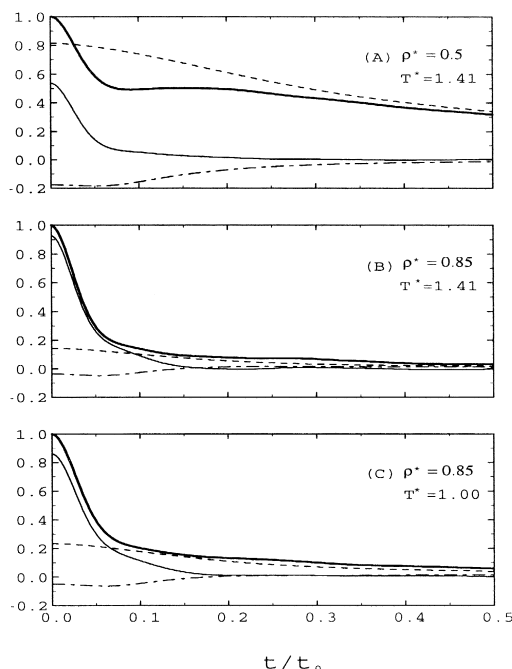


Fig. 3. Components of the $C(t)$ functions shown in Fig. 1. In each plot, the bold solid line is for $C(t)$, the thin solid line for $C_{\text{in-in}}(t)$, the dashed line for $C_{\text{out-out}}(t)$, and the dash-dotted line for $C_{\text{in-out}}(t)$.

cles inside and outside the division; $\rho_{\text{solv}}^{\text{in-out}}(\omega)$ and $\rho_{\text{solv}}^{\text{out-in}}(\omega)$ are the two equal cross-terms for solvent particles in the two different regions. It is easy to prove that the total solvation spectrum is a sum of the four spectra, and the square of the solvation frequency, ω_{solv}^2 , which is proportional to the area of $\rho_{\text{solv}}(\omega)$, is also a sum of the corresponding quantities of the four spectra¹.

The components of the $C(t)$ functions for the ‘epsilon’ model at three thermodynamic states are shown in Fig. 3. From Figs. 2 and 3, it is obvious that the initially ultrafast decay of $C(t)$ is resulted from the inertial motions of solvent particles inside the solvent cage. The time scale of this ultrafast component is of the order of the times for those

¹ The integral over the cross-term solvation spectrum between the inside and outside solvents is, in general, not zero, though small.

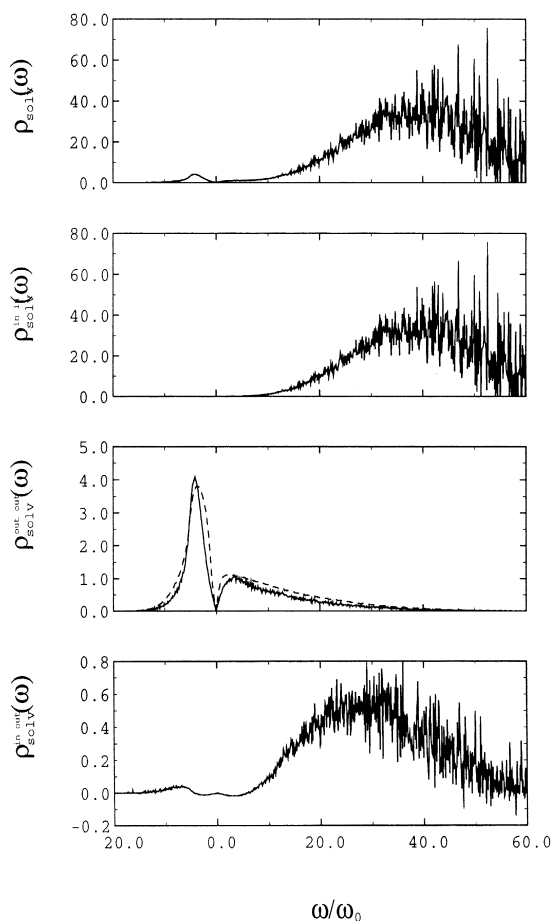


Fig. 4. Solvation spectrum and its components of the 'epsilon' model at $\rho^* = 0.5$ and $T^* = 1.41$. The dashed line in (C) is the INM DOS, multiplied by a constant, of the neat LJ fluid at the same thermodynamic condition. $\omega_0 = t_0^{-1}$

solvent particles being repelled out of the cage by the solute. The slow component of $C(t)$ is, in general, due to the solvent particles outside the cage. For the low-density solvent ($\rho^* = 0.5$) with a less rigid structure, the slow component of $C(t)$ is much longer. An important point is that the bump in $C(t)$ at $\rho^* = 0.5$ is resulted from the $C_{\text{in-out}}(t)$ component, which is almost flat at short times and increases monotonically roughly in the time scale of the bump, which is also the time scale of the outward expansion of the solvent particles originally near r_m . This comparison gives another indication that it is the

expansion of the solvent cage that gives rise to the bump in $C(t)$ observed in this low-density fluid. This explanation is consistent with the fact that no bump is observed in the high-density solvents ($\rho^* = 0.85$). Since the solvent cage in a high-density fluid is much rigid, the increase in $C_{\text{in-out}}(t)$ is too small to cause a bump in $C(t)$, but only make the tail of $C(t)$ a little longer.

The solvation spectrum and its components for the fluid at $\rho^* = 0.5$ and $T^* = 1.41$ are shown in Fig. 4. At this state, the total spectrum $\rho_{\text{solv}}(\omega)$ is almost identical with $\rho_{\text{solv}}^{\text{in-in}}(\omega)$, except for the small differences in the low-frequency part of the real-frequency lobe and in the imaginary-frequency lobe. This result gives the evidence that the short-time dynamics of solvation is determined by those solvent particles inside the cage. The shape of $\rho_{\text{solv}}^{\text{out-out}}(\omega)$ is quite similar as that of the INM DOS of the simple LJ fluid at the same thermodynamic condition. Compared with $\rho_{\text{solv}}^{\text{in-in}}(\omega)$ and $\rho_{\text{solv}}^{\text{out-out}}(\omega)$, the magnitudes of $\rho_{\text{solv}}^{\text{in-out}}(\omega)$ is very small, which indicates that the cage is indeed a good division so that the motions of the solvent particles inside and outside the cage do not have much correlation initially. The contributions to the square of the solvation frequency, which are calculated from the area of the solvation spectra, are given in Table 1. For the three thermodynamic states we simulated, about 95% of the contribution to ω_{solv}^2 comes from the solvent particles inside the cage. We show in Fig. 5 the comparisons of the linearized INM solvation theory for the components of the $C(t)$ function with the MD simulation results. In general, the predictions of the linearized INM solvation theory agree with the simulation results only as the solvent particles initially inside the cage have yet penetrated through the cage.

Table 1
Contributions to ω_{solv}^2 for the 'epsilon' model at three different thermodynamic states

Contributions to ω_{solv}^2 (unit in ω_0^2)	$\rho^* = 0.5$ $T^* = 1.41$	$\rho^* = 0.85$ $T^* = 1.41$	$\rho^* = 0.85$ $T^* = 1.00$
from all solvents	730.6	1022.2	900.7
from solvents inside the cage	691.1	987.2	852.0
from solvents outside the cage	20.3	10.5	17.0
from the two cross-terms	21.2	24.6	31.6

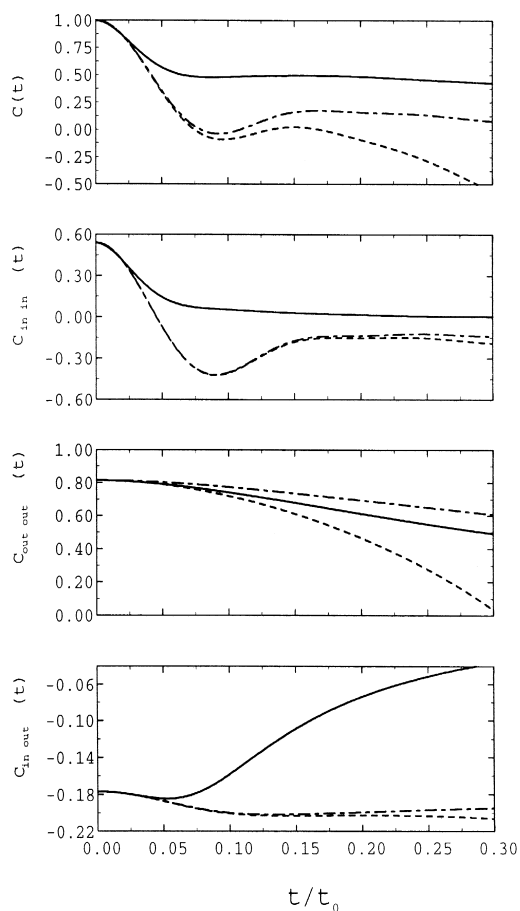


Fig. 5. Comparison of the linearized INM solvation theory for the components of $C(t)$ with the MD simulation results (solid lines) for the ‘epsilon’ model at $\rho^* = 0.5$ and $T^* = 1.41$. The dashed lines are calculated in terms of Eq. (5) with the full solvation spectra shown in Fig. 4, and the dot-dashed lines with the real-frequency spectra only.

A point is worth noticing is that the INM approximation of $C_{in-out}(t)$ deviates from the MD simulation results almost at the time as the function starts to increase, which is of the order of the time for the solvent-cage expansion.

4. Conclusion

In this Letter, through studying a bump observed in the solvation time correlation function of the ‘epsilon’ model at the time scale right after the

ultrafast decay component, we have proposed a possible nonpolar solvation mechanism – the solvent-cage expansion – at an intermediate time scale. By our definition, a metastable solvent cage around a solute is composed of those solvent particles near the first maximum of the solute-solvent radial distribution function where the mean forces on those particles are almost zero. The expansion of the solvent cage is caused by the impulses from the solvent particles, which were originally inside the cage but are repelled out of the cage by the strong repulsive forces due to the solute. Our results indicate that the time scale for the solvent-cage expansion is intermediate between those of inertial motions and structural relaxation. The physical picture of the solvent-cage expansion is similar, in some aspects, as the viscoelastic continuum solvation model [18], in which nonpolar solvation dynamics is described as the expansion or contraction of the solute-occupied cavity from an equilibrated size in the ground state to a new one in the excited state. However, according to our analyses, the cavity, or the solvent cage, should not survive infinitely, but will break up through diffusion processes at some time.

Acknowledgements

T.M.W. would like to acknowledge support from the National Science Council of Taiwan, ROC under Grand No. NSC 89-2112-M-009-009.

References

- [1] J.T. Fourkas, M. Berg, *J. Chem. Phys.* 98 (1993) 7773.
- [2] J.T. Fourkas, A. Benigno, M. Berg, *J. Chem. Phys.* 99 (1993) 8552.
- [3] D.S. Larsen, K. Ohta, G.R. Fleming, *J. Chem. Phys.* 111 (1999) 8970.
- [4] M.L. Horng, J.A. Gardecki, A. Papazyan, M. Maroncelli, *J. Phys. Chem.* 99 (1995) 17311.
- [5] R.M. Stratt, M. Maroncelli, *J. Phys. Chem.* 100 (1996) 12981.
- [6] J.G. Saven, J.L. Skinner, *J. Chem. Phys.* 99 (1993) 4391.
- [7] M.D. Stephens, J.G. Saven, J.L. Skinner, *J. Chem. Phys.* 106 (1997) 2129.
- [8] T. Yamaguchi, Y. Kimura, N. Hirota, *J. Chem. Phys.* 111 (1999) 4169.

- [9] T.M. Wu, S.L. Chang, *Phys. Rev. E* 59 (1999) 2993.
- [10] R.M. Stratt, *Acc. Chem. Res.* 28 (1995) 201.
- [11] T. Keyes, *J. Phys. Chem. A* 101 (1997) 2921.
- [12] A.L. Harris, J.K. Brown, C.B. Harris, *Annu. Rev. Phys. Chem.* 39 (1988) 341.
- [13] S.W. Hann, *Phys. Rev. A* 20 (1979) 2516.
- [14] R.M. Stratt, M. Cho, *J. Chem. Phys.* 100 (1994) 6700.
- [15] B.M. Ladanyi, R.M. Stratt, *J. Phys. Chem.* 99 (1995) 2502.
- [16] R.E. Larsen, E.F. David, G. Goodyear, R.M. Stratt, *J. Chem. Phys.* 107 (1997) 524.
- [17] R.E. Larsen, R.M. Stratt, *Chem. Phys. Lett.* 297 (1998) 211.
- [18] M. Berg, *J. Phys. Chem. A* 102 (1998) 17.